JVI Journals.ASM.org

Wongabel Rhabdovirus Accessory Protein U3 Targets the SWI/SNF Chromatin Remodeling Complex

D. Albert Joubert,[a]* Julio Rodriguez-Andres,[a] Paul Monaghan,[a] Michelle Cummins,[a] William J. McKinstry,[c] Prasad N. Paradkar,[a] Gregory W. Moseley,[b] Peter J. Walker[a]

CSIRO Biosecurity, Australian Animal Health Laboratory, Geelong, VIC, Australia[a]; Department of Biochemistry and Molecular Biology, Bio21 Institute, University of Melbourne, Melbourne, VIC, Australia[b]; CSIRO Materials Science and Engineering, Parkville, VIC, Australia[c]

ABSTRACT

Wongabel virus (WONV) is an arthropod-borne rhabdovirus that infects birds. It is one of the growing array of rhabdoviruses with complex genomes that encode multiple accessory proteins of unknown function. In addition to the five canonical rhabdovirus structural protein genes (N, P, M, G, and L), the 13.2-kb negative-sense single-stranded RNA (ssRNA) WONV genome contains five uncharacterized accessory genes, one overlapping the N gene (Nx or U4), three located between the P and M genes (U1 to U3), and a fifth one overlapping the G gene (Gx or U5). Here we show that WONV U3 is expressed during infection in insect and mammalian cells and is required for efficient viral replication. A yeast two-hybrid screen against a mosquito cell cDNA library identified that WONV U3 interacts with the 83-amino-acid (aa) C-terminal domain of SNF5, a component of the SWI/SNF chromatin remodeling complex. The interaction was confirmed by affinity chromatography, and nuclear colocalization was established by confocal microscopy. Gene expression studies showed that SNF5 transcripts are upregulated during infection of mosquito cells with WONV, as well as West Nile virus (*Flaviviridae*) and bovine ephemeral fever virus (*Rhabdoviridae*), and that SNF5 knockdown results in increased WONV replication. WONV U3 also inhibits SNF5-regulated expression of the cytokine gene *CSF1*. The data suggest that WONV U3 targets the SWI/SNF complex to block the host response to infection.

IMPORTANCE

The rhabdoviruses comprise a large family of RNA viruses infecting plants, vertebrates, and invertebrates. In addition to the major structural proteins (N, P, M, G, and L), many rhabdoviruses encode a diverse array of accessory proteins of largely unknown function. Understanding the role of these proteins may reveal much about host-pathogen interactions in infected cells. Here we examine accessory protein U3 of Wongabel virus, an arthropod-borne rhabdovirus that infects birds. We show that U3 enters the nucleus and interacts with SNF5, a component of the chromatin remodeling complex that is upregulated in response to infection and restricts viral replication. We also show that U3 inhibits SNF5-regulated expression of the cytokine colony-stimulating factor 1 (CSF1), suggesting that it targets the chromatin remodeling complex to block the host response to infection. This study appears to provide the first evidence of a virus targeting SNF5 to inhibit host gene expression.

The *Rhabdoviridae* family is one of the most ecologically diverse families of RNA viruses, with members infecting plants, vertebrates, and invertebrates. The negative-sense single-stranded RNA (ssRNA) genomes of known rhabdoviruses range in size from ~11 kb to 16 kb (1; P. J. Walker, C. Firth, S. G. Widen, K. R. Blasdell, H. Guzman, T. G. Wood, P. N. Paradkar, E. C. Holmes, R. B. Tesh, and N. Vasilakis, submitted for publication). All the genomes contain five genes, arranged in the order 3′-N-P-M-G-L-5′, encoding structural proteins with functional characteristics that are very well described. However, in many rhabdoviruses, the structural protein genes are interspersed, overprinted, or overlapped, with "accessory" genes encoding proteins that are unrelated to other viral or host proteins and have functions that are either poorly understood or entirely unknown (1). As observed for other RNA viruses (such as paramyxoviruses, coronaviruses, and lentiviruses), rhabdovirus accessory genes may encode proteins with important functions in virus replication, pathogenesis, and evasion of host responses to infection (1–4). Furthermore, as many plant and animal rhabdoviruses are transmitted by replication in insect vectors, some may play a role in the invertebrate host, in which the processes of infection, persistence, and immunity are poorly understood (1, 5).

Wongabel virus (WONV) was isolated in 1979 from biting midges (*Culicoides austropalpalis*) collected near Kairi in Queensland, Australia (6). It is currently classified as an unassigned species (*Wongabel virus*) of the family *Rhabdoviridae*. WONV-neutralizing antibodies have been detected in sea birds collected from the Great Barrier Reef, but there is no evidence to date that the virus is associated with human or animal disease (7). The 13,196-nucleotide (nt) genome is relatively complex, encoding five putative accessory proteins (WONV U1 to WONV U5) of unknown

Received 10 July 2014 **Accepted** 7 November 2014

Accepted manuscript posted online 12 November 2014

Citation Joubert DA, Rodriguez-Andres J, Monaghan P, Cummins M, McKinstry WJ, Paradkar PN, Moseley GW, Walker PJ. 2015. Wongabel rhabdovirus accessory protein U3 targets the SWI/SNF chromatin remodeling complex. J Virol 89:1377–1388. doi:10.1128/JVI.02010-14.

Editor: D. S. Lyles

Address correspondence to Peter J. Walker, Peter.Walker@csiro.au.

* Present address: D. Albert Joubert, School of Biological Sciences, Monash University, Clayton, VIC, Australia.

D.A.J. and J.R.-A. contributed equally to the study.

doi:10.1128/JVI.02010-14

function (6). Open reading frames (ORFs) U1, U2, and U3 are arranged consecutively between the P and M genes, encoding small acidic proteins (~16.5 to ~21.9 kDa) with low but identifiable sequence homology (1). WONV U4 (or Nx) lies in a second consecutive ORF in the N gene and encodes a putative ~5.8-kDa protein. ORF U5 (or Gx) overlaps the G gene and encodes a putative ~14.9-kDa protein with structural characteristics similar to the ephemerovirus viroporin-like α1 proteins (1, 6; Walker et al., submitted).

In this paper, we investigate the function of the ~16.5-kDa WONV U3 protein. We demonstrate that WONV U3 is expressed during infection of mammalian and insect cells and is required for efficient viral replication. We also show that WONV U3 is translocated to the nucleus, where it binds to SNF5, a component of the SWI/SNF chromatin remodeling complex, inhibiting SNF5-regulated gene expression. This strategy may be used by the virus to inhibit the host response to viral infection.

MATERIALS AND METHODS

Virus propagation and titration. WONV (CS264 strain), bovine ephemeral fever virus (BEFV) (CS1865 strain), and West Nile virus (WNV) (Kunjin K42886 strain) were propagated in African green monkey kidney (Vero or COS-7), baby hamster kidney (BHK-BSR), or *Aedes albopictus* (C6/36) cell lines. Mammalian cells were cultivated as described previously (9, 10). Insect cells were grown at 32°C in 199 medium supplemented with 10 mM HEPES, 2 mM L-glutamine, 137 μM streptomycin, 80 U/ml penicillin, and 5% fetal calf serum. Fifty percent tissue culture infective dose ($TCID_{50}$) titrations were conducted in Vero cells, and titers were estimated according to the method of Reed and Muench (11).

RNA and protein extractions. Total RNA was extracted by using the RNeasy Plus minikit (Qiagen) according to the manufacturer's specifications. Unless otherwise stated, protein extractions were conducted by washing cells once with phosphate-buffered saline (PBS) followed by ice-cold buffer I (10 mM Tris-HCl [pH 7.5], 10 mM NaCl, 10 mM EDTA, 0.5% Triton X-100, 5 mM dithiothreitol [DTT], 1× Sigma P2714 protease inhibitor). The cell suspension was adjusted to a final concentration of 150 mM NaCl, passed five times through a 20-gauge needle, agitated for 30 min at 4°C, and centrifuged at 1,500 × *g* for 15 min. The clarified lysate was stored at −20°C.

Cloning and expression of WONV U3 for purification from *E. coli*. The WONV U3 ORF was cloned into the NheI and BamHI sites of a modified pET43 vector (Novagen) in which the NusA solubility tag was replaced with a C-terminal hexahistidine tag (pETCSIRO-B). The construct was transformed into *Escherichia coli* strain Rosetta, and the expressed protein was purified by using a HisTRAP FF immobilized Ni^{2+} affinity column (GE Healthcare), as described previously (12).

Yeast two-hybrid screen. Yeast two-hybrid screens were conducted by using the Matchmaker Gold yeast two-hybrid system (Clontech) according to the manufacturer's specifications. To construct the bait plasmid, the WONV U3 ORF was amplified by PCR using gene-specific primers. The PCR product was cloned into the BamHI and SalI sites of pGBKT7 to yield pGBKT7(WU3), and the construct was confirmed by sequencing.

To construct the target library, C6/36 cells were infected with BEFV, and RNA was extracted at 0, 12, 24, 36, and 72 h postinfection (hpi). Pooled RNA from all extractions was used to construct the library by using the Mate & Plate library system (Clontech) according to the manufacturer's specifications. All subsequent two-hybrid matings and screenings were conducted according to the specifications of the Matchmaker Gold yeast two-hybrid system (Clontech).

Full-length *Aedes albopictus* SNF5 (AaSNF5) was amplified from the C6/36 library, and full-length *Homo sapiens* SNF5 was amplified from cDNA prepared from HeLa cells by using gene-specific primers. Each amplified sequence was cloned into the BamHI/BglII and SalI sites of pGADT7 to yield pGADT7(AaSNF5) and pGADT7(HsSNF5), respectively. The full-length constructs were subsequently used for all yeast two-hybrid analyses between WONV U3 and AaSNF5.

Cloning of fluorescent fusion proteins. The WONV U3 ORF was cloned into the EcoRI and SalI sites of pAcGFP1-C2 (Clontech) to yield pAcGFP1-C2(WU3) for expression of WONV U3 fused at its N terminus to green fluorescent protein (GFP). Plasmid pEGFP-C1-RVP-P1 was described previously (13). For expression of red fluorescent protein (RFP)-fused proteins, the GFP ORF of pAcGFP1-C2 was replaced with the RFP ORF, which was excised from pmCherry-C1 by using NheI and BsrGI; this generated the pAcRFP-C2 vector. The partial SNF5 ORF (84 amino acids [aa]) obtained from the yeast two-hybrid screen was cloned into this vector by using BglII and SalI to produce pAcRFP-C2(SNF5).

Transfections. Transfections for overexpression of WONV U3 were conducted in 6-well plates by using 2 μg plasmid DNA and Lipofectamine 2000 (Invitrogen) (1:2) according to the manufacturer's specifications. Transfections for confocal microscopy were conducted as described below, in 24-well plates containing glass coverslips. For knockdown experiments, transfections were conducted by using 1.5 μg small interfering RNA (siRNA) and Lipofectamine 2000 for Vero and BHK/BSR cells and Cellfectine II (Invitrogen) for C6/36 cells, according to the manufacturer's specifications. Luciferase siRNA (siRNA[Luc]) (Invitrogen) was used as a nonspecific knockdown control.

Preparation of antisera. Polyclonal WONV U3 antiserum was raised in 3-week-old specific-pathogen-free (SPF) White Leghorn chickens (Spafas). For primary immunization and boosts, each chicken was injected intramuscularly at 2-week intervals with 50 μg WONV U3. The first dose was prepared in CSIRO triple adjuvant (60% [vol/vol] Montanide combined with 3 mg/ml Quil A and 30 mg/ml DEAE-dextran in PBS). The second and third boosts were prepared in Freund's incomplete adjuvant in PBS. Sera were collected following each immunization. Antibody titers were determined by an enzyme-linked immunosorbent assay (ELISA) against the immunizing antigen.

Immunoblotting. Protein extracts were treated and analyzed by SDS-PAGE and immunoblotting as described previously (10). Primary antibodies (anti-WU3 chicken serum, anti-GFP mouse serum, and anti-SNF5 mouse serum) and secondary antibodies (rabbit anti-chicken horseradish peroxidase [HRP]-conjugated IgY and sheep anti-mouse HRP-conjugated IgG; Thermofisher) were used at a dilution of 1/2,000.

Laser scanning confocal microscopy. Transfected cells were fixed in 4% paraformaldehyde in PBS at room temperature for 40 min and then washed and stored in PBS at 4°C. Nuclei were labeled with 4′,6-diamidino-2-phenylindole (DAPI) (Sigma) in distilled H_2O, and the coverslips were mounted on microscope slides in Vectashield (Vector Laboratories), sealed, and imaged by using a Leica Microsystems SP5 confocal microscope with a 60× oil immersion objective. Cell monolayers were treated with 0.1% Triton X-100 for 10 min. Nonspecific binding was then blocked in 0.5% PBS for 30 min. Primary antibody diluted in 0.5% bovine serum albumin (BSA) in PBS (1/750 for SNF5 antibody and 1/500 for anti-WU3 chicken serum) was added, and the cells were incubated for 1 h, washed, and incubated with secondary antibody in 0.5% BSA in PBS (1/200 for Alexa Fluor 568 goat anti-rabbit for SNF5 and Alexa Fluor 488 goat anti-chicken for U3). Monolayers were then washed in PBS and rinsed with distilled H_2O. Nuclei were then labeled with DAPI in distilled H_2O, and the coverslips were mounted onto microscope slides, sealed, and imaged by using a Leica Microsystems SP5 confocal microscope with a 60× oil immersion objective.

To assess nuclear trafficking in live cells, transfected COS-7 cells were treated with 2.8 ng/ml leptomycin B (LMB) for 3 h before imaging using an inverted Nikon C1 confocal microscope with a 100× oil immersion objective and a heated stage. To determine the nucleocytoplasmic localization of protein, the ratio of nuclear to cytoplasmic fluorescence (Fn/c) was calculated from digitalized images of >30 transfected cells by using Image J software, as described previously (13).

TABLE 1 Synthetic oligonucleotides used for generation of double-stranded siRNA

Organism	Target gene	Synthetic oligonucleotide for siRNA preparation[a]
Wongabel virus	N	GGATCCTAATACGACTCACTATAggtgataaaccaaaacctc
		AAgaggttttggttttatcaccTATAGTGAGTCGTATTAGGATCC
		GGATCCTAATACGACTCACTATAgaggttttggtttatcacc
		AAggtgataaaccaaaacctcTATAGTGAGTCGTATTAGGATCC
		GGATCCTAATACGACTCACTATAgaattcttcgagaaaaatc
		AAgatttttctcgaagaattcTATAGTGAGTCGTATTAGGATCC
		GGATCCTAATACGACTCACTATAgatttttctcgaagaattc
		AAgaattcttcgagaaaaatcTATAGTGAGTCGTATTAGGATCC
Wongabel virus	U3	GGATCCTAATACGACTCACTATAgactagacgagtgtatttc
		AAgaaatacactcgtctagtcTATAGTGAGTCGTATTAGGATCC
		GGATCCTAATACGACTCACTATAgaaatacactcgtctagtc
		AAgactagacgagtgtatttcTATAGTGAGTCGTATTAGGATCC
		GGATCCTAATACGACTCACTATAgtgaagaaatcctggaccc
		AAgggtccaggatttcttcacTATAGTGAGTCGTATTAGGATCC
		GGATCCTAATACGACTCACTATAgggtccaggatttcttcac
		AAgtgaagaaatcctggacccTATAGTGAGTCGTATTAGGATCC
Aedes albopictus	SNF5	GGATCCTAATACGACTCACTATAgaagaacgcaagaagctgc
		AAgcagcttcttgcgttcttcTATAGTGAGTCGTATTAGGATCC
		GGATCCTAATACGACTCACTATAgaaatacactcgtctagtc
		AAgcagcttcttgcgttcttcTATAGTGAGTCGTATTAGGATCC
		GGATCCTAATACGACTCACTATAggtgcacaacaagaagatc
		AAgatcttcttgttgtgcaccTATAGTGAGTCGTATTAGGATCC
		GGATCCTAATACGACTCACTATAgatcttcttgttgtgcacc
		AAggtgcacaacaagaagatcTATAGTGAGTCGTATTAGGATCC

[a] Gene-specific sequences are underlined and in lowercase type.

Affinity chromatography. The 84-aa C-terminal domain of AaSNF5 was cloned downstream of *E. coli* maltose binding protein (MBP) by using the vector pMALc5x (New England BioLabs), transformed into *E. coli* NEBexpress (New England BioLabs), and inoculated into 250 ml of LB supplemented with 100 μg/ml ampicillin and 0.2% glucose. The culture was grown at 37°C to an optical density at 600 nm (OD_{600}) of 0.6 before induction with 0.3 mM isopropyl-β-D-thiogalactopyranoside (IPTG) at 22°C for 24 h. The cells were then harvested by centrifugation at 16,000 × *g* for 10 min at 4°C, resuspended in 10 ml buffer II (20 mM Tris-HCl [pH 7.5], 200 mM NaCl, 1 mM EDTA) containing 5 mM DTT and Sigma P2714 protease inhibitor (200 mM buffer II-DP), frozen at −20°C, and thawed on ice. The suspension was then sonicated for 1 min in 15-s pulses, clarified by centrifugation at 16,000 × *g* for 20 min at 4°C, and added to 1 ml amylose resin (New England BioLabs) washed in 5 volumes of buffer II. The slurry was incubated with gentle rotation for 4 h, centrifuged at 8,000 × *g* for 10 min, resuspended in 1 ml 200 mM buffer II-DP, transferred into an Eppendorf tube, and washed with 10 volumes of the same buffer. Slurries containing either MBP or MBP-AaSNF5 bound to amylose were used for pulldown assays.

A crude protein lysate (~5 mg/ml) from WONV-infected Vero cells was preadsorbed for 2 h at 4°C with amylose resin prewashed in buffer II. The resin was then removed by centrifugation, and the lysate was made up to 10 ml with buffer II containing 150 mM NaCl, 5 mM DTT, and 1× Sigma P2714 protease inhibitor (150 mM buffer II-DP). Equal aliquots of the lysate were then treated with amylose resin containing MBP or MBP-SNF5 at 4°C for 24 h with gentle agitation. The resin was then recovered by centrifugation at 5,000 × *g* at 4°C, resuspended in 1 ml of ice-cold 150 mM buffer II-DP, washed with 10 volumes of the same ice-cold buffer, resuspended in 200 μl of 2× loading buffer, and analyzed by SDS-PAGE and immunoblotting.

BHK-BSR cells were transfected with either pAcGFP1-C2 or pAcGFP1-C2(WU3) and 2 μl of Lipofectamine 2000 in a 6-well plate. At 24 h posttransfection, cells were pelleted, and GFP trapping was conducted by using a GFP-Trap_M kit (Chromotek) according to the manufacturer's instructions. Cell pellets were resuspended in 200 μl lysis buffer by pipetting and incubated on ice for 30 min. The resulting lysates were centrifuged at 20,000 × *g* for 10 min at 4°C, and the supernatant was transferred into a prechilled tube. An equilibrated GFP-Trap_M bead slurry (30 μl) was added and allowed to mix with the lysate for 2 h at room temperature. The beads were separated magnetically, and the supernatant was discarded. The beads were then washed twice with 500 μl ice-cold wash buffer. In order to disassociate the beads, 2× SDS sample buffer was added, and the samples were heated at 95°C for 10 min. The samples were then analyzed by SDS-PAGE (Invitrogen) as described above.

Double-stranded siRNA preparation. Double-stranded siRNAs against AaSNF5, WONV N, and WONV U3 were synthesized from synthetic oligonucleotides containing a T7 promoter sequence (Table 1). Single-stranded oligonucleotides were synthesized by Geneworks Australia. The oligonucleotides were resuspended in water, and complementary strands were mixed, heated at 75°C for 30 min, and then allowed to cool at room temperature overnight. This template was used to synthesize double-stranded siRNA by using the mMESSAGE mMACHINE T7 Ultra kit (Ambion, Australia). Double-stranded siRNAs against mammalian SNF5 were ordered from Millennium Science (Thermo Scientific) and used according to the manufacturer's specifications by using siRNA delivery medium (Thermo Scientific). siRNA against *Renilla* luciferase (also provided by Millennium Science) was used as a control.

Quantitative real-time PCR. Quantitative real-time PCR (qRT-PCR) was performed by using SYBR green PCR master mix (Invitrogen, Australia). Total RNA was used to prepare cDNA by using SuperScript III reverse transcriptase (Invitrogen, Australia) and random hexamer primers according to the manufacturer's specifications. qRT-PCR was performed by using ~20 ng cDNA and gene-specific primers. Cycle conditions were a denaturation step at 95°C for 10 min and 45 cycles of 95°C for 15 s and 60°C for 1 min. Copy numbers were determined by constructing standard curves, and fold induction profiles were determined by using the $\Delta\Delta C_T$ method (14). cDNA normalization was conducted by using internal 18S (Vero and BHK-BSR cells) or 17S (C6/36 cells) RNA primers.

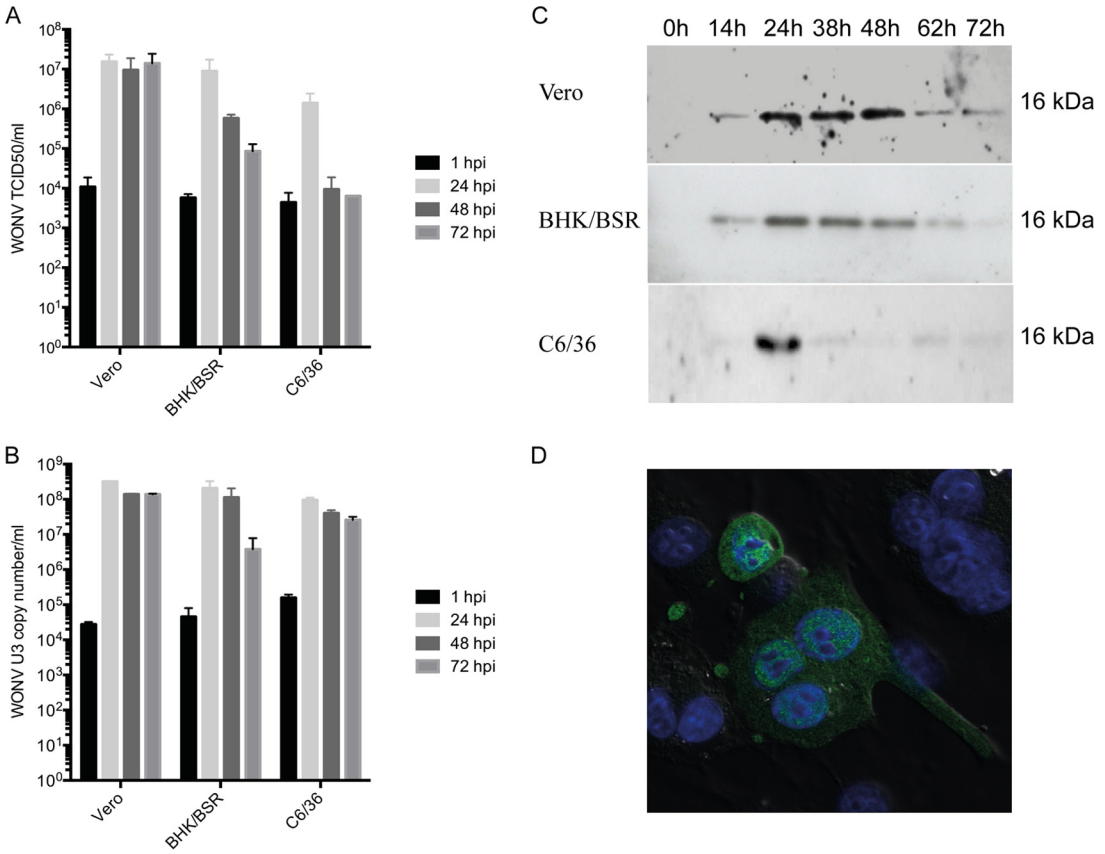

FIG 1 WONV U3 expression in mammalian and insect cells. (A) $TCID_{50}$ titers at 0, 24, 48, and 72 hpi in Vero, BHK-BSR, and C6/36 cells infected with WONV at 1 $TCID_{50}$/cell. (B) Copy number determined by qRT-PCR of WONV U3 mRNA following WONV infection at 1 $TCID_{50}$/cell of Vero, BHK-BSR, and C6/36 cells. (C) Immunoblot detection of WONV U3 protein in Vero (top), BHK-BSR (middle), and C6/36 (bottom) cells infected with WONV at 1 $TCID_{50}$/cell. (D) Detection by indirect immunofluorescence of WONV U3 protein expression in BHK-BSR cells following infection with WONV at 1 $TCID_{50}$/cell (blue, DAPI; green, WONV U3).

Nucleotide sequence accession number. The GenBank accession number for the *Aedes albopictus* SNF5 gene is KC576842.

RESULTS

WONV U3 is expressed during WONV infection in insect cells and mammalian cells. WONV U3 gene expression was analyzed during the course of infection in mammalian (Vero and BHK-BSR) and insect (C6/36) cells. Cells were infected with WONV (multiplicity of infection [MOI] of 1 $TCID_{50}$/cell), and mRNA and protein expression levels were determined at various times postinfection by qRT-PCR and immunoblotting, respectively.

In Vero and BHK-BSR cells, WONV infection resulted in a progressive cytopathic effect (CPE). In Vero cells, virus titers reached ~10^7 $TCID_{50}$/ml by 24 hpi and remained high up to 72 hpi, when there was total destruction of the cell monolayer (Fig. 1A). WONV U3 mRNA levels peaked at 24 hpi and declined by ~5-fold at 72 hpi (Fig. 1B). BHK-BSR cells exhibited a CPE similar to that of Vero cells, and virus titers reached similarly high levels, but in contrast to Vero cells, WONV titers declined sharply (~2 logs) by 72 hpi (Fig. 1A). WONV U3 mRNA levels similarly peaked at 24 hpi but declined sharply (~1.5 logs) at 72 hpi. WONV U3 protein levels were detected in Vero and BHK-BSR cells from 14 hpi, peaked at 24 to 48 hpi and then declined as the CPE progressed (Fig. 1C). WONV U3 was also detected in BHK-BSR cells by immunofluorescence and was localized predominantly in the nucleus (Fig. 1D).

WONV infection in C6/36 cells resulted in almost no visible CPE, and cells recovered from an initial disturbance to display a normal appearance by 72 hpi. WONV titers were significantly lower than those observed in Vero and BHK-BSR cells. Titers in C6/36 cells peaked at ~1×10^6 $TCID_{50}$/ml at 24 hpi and then declined by 48 hpi to stabilize at ~8×10^3 $TCID_{50}$/ml at 72 hpi (Fig. 1A). WONV U3 mRNA expression levels were also lower in C6/36 cells but displayed a pattern similar to that observed in Vero cells. Viral mRNA copy numbers peaked at 24 hpi and then diminished 3-fold to 5-fold at 72 hpi (Fig. 1B). The pattern of viral protein expression in C6/36 cells varied. Reflecting WONV titers, WONV U3 protein levels peaked sharply at 24 hpi and then declined sharply (Fig. 1C).

WONV U3 is required for efficient viral replication. Knockdown experiments were conducted to determine if WONV U3 expression is required for efficient viral replication in cell culture by using double-stranded siRNAs targeting WONV N gene (siRNA[N]) and U3 gene (siRNA[WU3]) transcripts. The specificity of the siRNAs for the knockdown of each target protein was established by using GFP fusion constructs expressed from transfected plasmids (Fig. 2). Vero cells were infected with WONV (MOI of 1 $TCID_{50}$/cell) and transfected at 6 hpi with siRNA[N] or

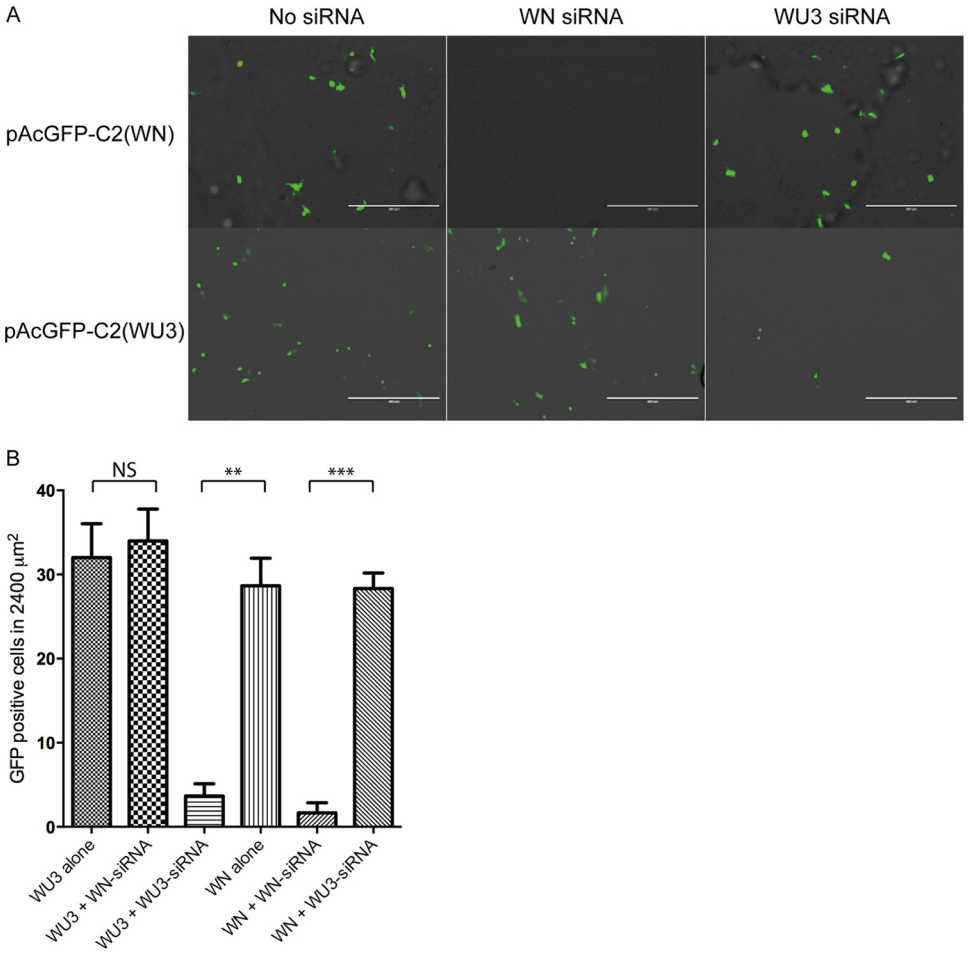

FIG 2 WONV U3 siRNA does not target plasmid-expressed WONV N mRNA. (A) Cells transfected with pAcGFP1-C2(WN) or pAcGFP1-C2(WU3) and WONV U3 siRNA (siRNA[U3]) or WONV N siRNA (siRNA [N]). Cells were fixed at 24 h posttransfection and observed by using an Evos FL microscope (Life Technologies). Bar, 400 μm. (B) GFP-positive cell count after transfection with pAcGFP1-C2(WN) or pAcGFP1-C2(WU3) and siRNA[U3] or WONV siRNA[N] on a 2,400-μm^2 surface. Positive cells were identified and quantified by using the Evos FL cell imaging system (Life Technologies). Statistical analyses were conducted by using an unpaired two-tailed Student *t* test with GraphPad Prism 6C. Significant differences are indicated (***, $P \leq 0.001$; **, $P \leq 0.01$; NS, not significant).

siRNA[WU3]. Treatment with siRNA[N] resulted in a 5-fold to 10-fold reduction in N mRNA levels at 24 to 72 hpi and a small but significant reduction in WONV U3 mRNA levels compared to those in cells treated with control siRNA[Luc] (Fig. 3A and B). Treatment of cells with siRNA[WU3] resulted in a significant reduction in WONV U3 mRNA levels and a generally smaller but significant reduction in N mRNA levels at 24 to 72 hpi (Fig. 3C and D). Viral infectivity assays indicated that the knockdown of the N gene and WONV U3 gene had a similar effect on WONV titers, with 100-fold to 1,000-fold reductions at 24 hpi and 48 hpi but not at 72 hpi (Fig. 3E). Furthermore, overexpression of WONV U3 led to an ~6.5-fold (0.8-log) increase in WONV titers at 48 h postinfection (Fig. 3F). The effect of overexpression was evident only at a low MOI (0.1 $TCID_{50}$/cell), most likely because natural (virus-derived) expression of U3 at a high MOI overwhelms the level of overexpression from the plasmid (Fig. 3G). The data indicated that both N gene and WONV U3 gene expressions are required for efficient virus replication.

WONV U3 interacts with SNF5. A yeast two-hybrid screen was conducted to identify cellular proteins that may interact with WONV U3. Initially, a cDNA target library was constructed from BEFV-infected C6/36 cells, and a bait plasmid was constructed by using an amplified full-length clone of the WONV U3 ORF. The screen identified a strong interaction with a 249-bp insert encoding the 83-aa C-terminal region of a 371-aa polypeptide with 96.5% amino acid sequence identity to *Aedes aegypti* SNF5 (SWI/SNF-related matrix-associated actin-dependent regulator of chromatin subfamily B member 1; GenBank accession number XM_001648944) (Fig. 4). The full-length *Aedes albopictus* SNF5 transcript was amplified and sequenced. We used a subsequent yeast two-hybrid assay to demonstrate the binding of WONV U3 to full-length AaSNF5. To rule out any nonspecific binding of either WONV U3 or AaSNF5 to components of the yeast two-hybrid system, all possible plasmid combinations were transformed into the two respective *Saccharomyces cerevisiae* strains, and the strains were subsequently mated and plated onto progressively more stringent media. AaSNF5 specifically interacted with WONV U3, and no nonspecific interactions occurred between either WONV U3 or AaSNF5 and components of the yeast two-hybrid system (Fig. 5A). We also repeated the yeast two-hybrid

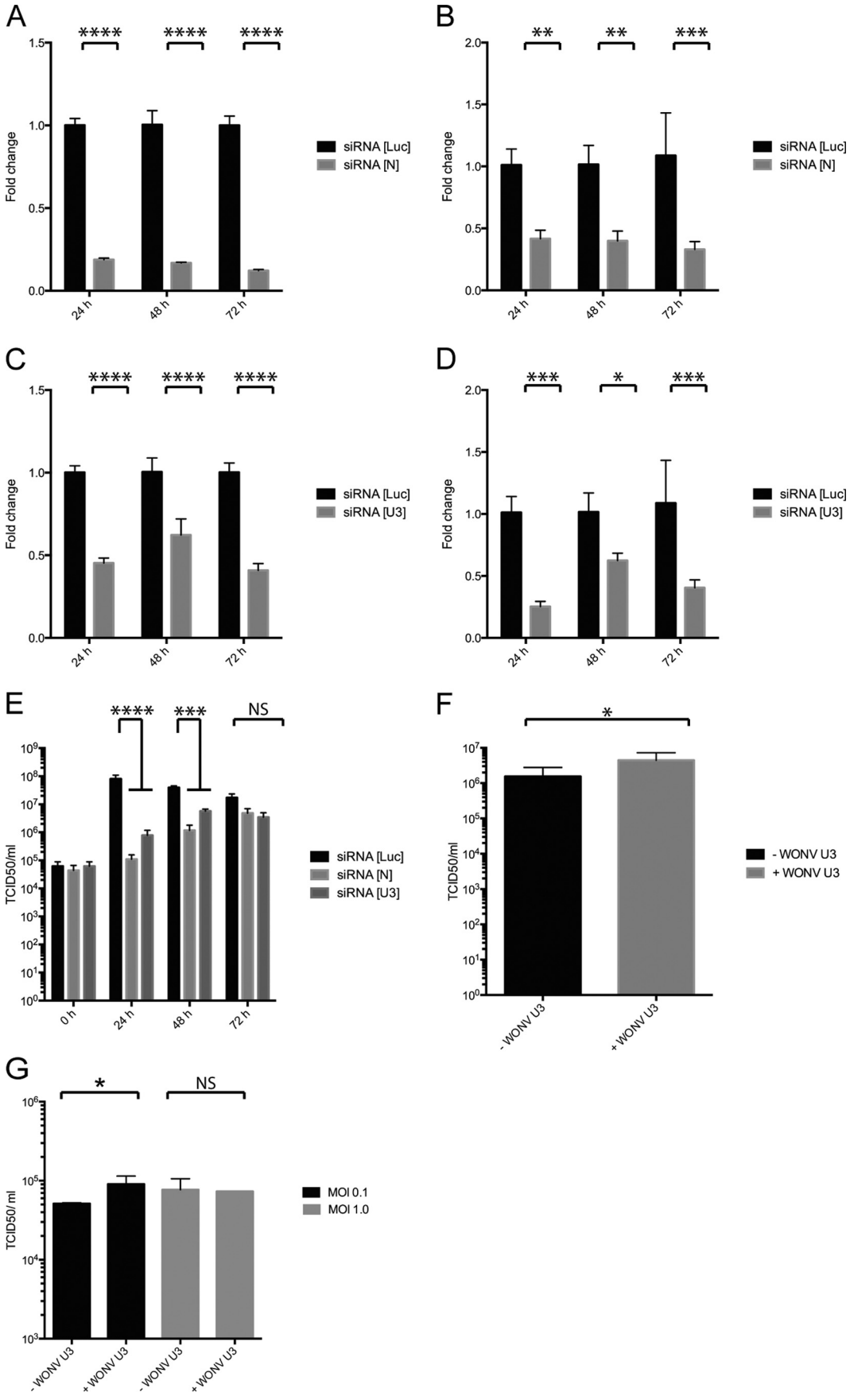
A
****
****
****
Fold change
1.5
1.0
0.5
0.0
24 h
48 h
72 h
siRNA [Luc]
siRNA [N]
B
**
**
***
Fold change
2.0
1.5
1.0
0.5
0.0
24 h
48 h
72 h
siRNA [Luc]
siRNA [N]
C
****
****
****
Fold change
1.5
1.0
0.5
0.0
24 h
48 h
72 h
siRNA [Luc]
siRNA [U3]
D
***
*
***
Fold change
2.0
1.5
1.0
0.5
0.0
24 h
48 h
72 h
siRNA [Luc]
siRNA [U3]
E
****
***
NS
TCID50/ml
10^9
10^8
10^7
10^6
10^5
10^4
10^3
10^2
10^1
10^0
0 h
24 h
48 h
72 h
siRNA [Luc]
siRNA [N]
siRNA [U3]
F
*
TCID50/ml
10^7
10^6
10^5
10^4
10^3
10^2
10^1
10^0
- WONV U3
+ WONV U3
- WONV U3
+ WONV U3
G
*
NS
TCID50/ ml
10^6
10^5
10^4
10^3
- WONV U3
+ WONV U3
- WONV U3
+ WONV U3
MOI 0.1
MOI 1.0

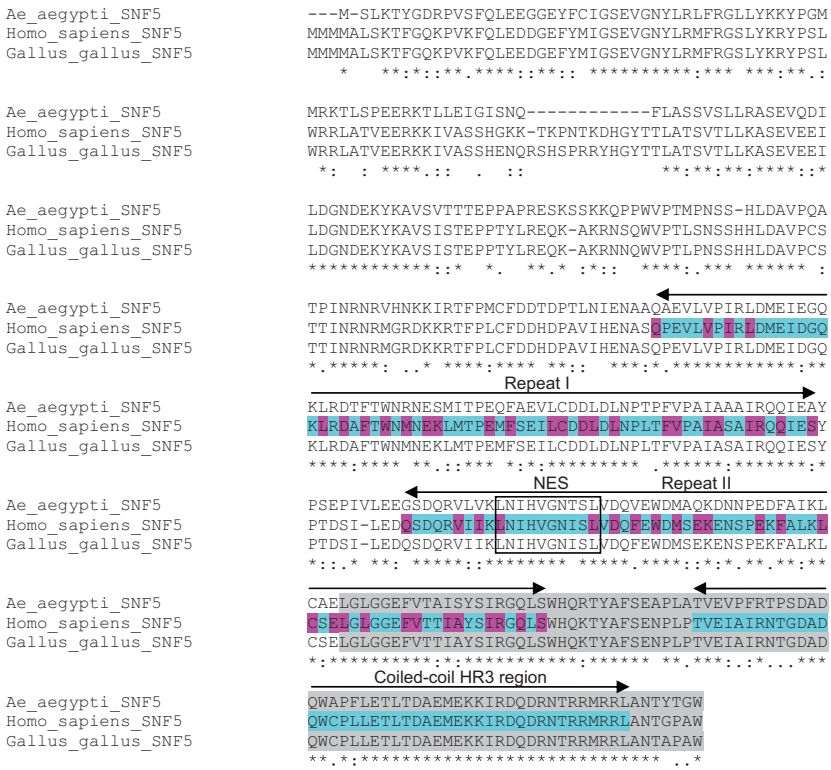

FIG 4 ClustalX alignment of the deduced amino acid sequences of mosquito (*Aedes albopictus* [GenBank accession number KC576842] and *Aedes aegypti* [accession number XM_001648944]), human (*Homo sapiens* [accession number AAA81905]), and chicken (*Gallus gallus* [accession number NP_001034344]) SNF5. Conserved domains are highlighted in blue. The predicted nuclear export signal is boxed. Conserved residues in the repeat domains are highlighted in purple. The 83-aa C-terminal region that has been shown to interact with WU3 is shaded in gray.

analysis with full-length mammalian SNF5 and obtained similar results (results not shown).

A GFP trap was employed to obtain independent confirmation of the interaction between WONV U3 and full-length SNF5. BHK-BSR cells were transfected with either pAcGFP1-C2 or pAcGFP1-C2(WU3). At 24 h posttransfection, clarified lysates were prepared and incubated with GFP binding proteins coupled to agarose beads. Proteins bound to the washed beads were eluted, resolved by SDS-PAGE, and examined by immunoblotting with antibodies specific to SNF5. As shown in Fig. 5B, SNF5 was detected in lysates transfected with pAcGFP1-C2(WU3) but not in lysates from cells transfected with the empty vector pAcGFP1-C2. The double band detected was observed in previous studies (15, 16) and is possibly due to the antibody detecting both SNF5 isoforms (Smarc1a and Smarc1b).

The 83-aa C-terminal domain of AaSNF5 was also cloned downstream of *E. coli* maltose binding protein (MBP). The MBP-AaSNF5 fusion protein was overexpressed, bound to amylose resin, and reacted with a lysate of WONV-infected Vero cells. As shown in Fig. 5C, a Western blot assay using WONV U3 antiserum detected specific binding of the fusion protein to the ~16-kDa WONV U3 protein.

WONV U3 colocalizes with SNF5 in the nucleus. The subcellular localization of WONV U3 was examined in BHK-BSR, Vero, and COS-7 cells by confocal microscopy. BHK-BSR cells were infected with WONV and stained for both WONV U3 (green) and SNF5 (red). WONV U3 and SNF5 were found to colocalize in the nucleus (Fig. 6A), but no clear direct association was detected. Further confirmation of this interaction was obtained by cotransfecting Vero cells with plasmid pAcRFP-C2(SNF5) expressing the 84-aa C-terminal region of AaSNF5 fused to RFP and plasmid pAcGFP1-C2(WU3) expressing full-length WONV U3 fused to GFP. Nuclear colocalization of the expressed fusion proteins was observed at 24 h posttransfection (Fig. 6B). The strong intranu-

FIG 3 Effects of WONV N gene knockdown (A, B, and E), WONV U3 gene knockdown (C to E), and WONV U3 gene overexpression (F and G) on WONV replication in Vero cells. (A) WONV N mRNA quantification by qRT-PCR following transfection with luciferase siRNA (siRNA[Luc]) or WONV N siRNA (siRNA[N]). (B) WONV U3 mRNA quantification by qRT-PCR following transfection with siRNA[Luc] or siRNA[N]. (C) WONV N mRNA quantification by qRT-PCR following transfection with siRNA[Luc] or siRNA directed against WONV U3 (siRNA[U3]). (D) WONV U3 mRNA quantification by qRT-PCR following transfection with siRNA[Luc] or siRNA[U3]. (E) WONV $TCID_{50}$ titration following transfection with siRNA[Luc], siRNA[N], or siRNA[U3]. (F and G) WONV titers in Vero cells transfected with the pAcGFP1-C2 vector (−WU3) or pAcGFP1-C2(WU3) expressing the WU3-GFP fusion protein (+WU3), infected with WONV at 24 h posttransfection, and assayed at 48 hpi. GFP expression was verified by fluorescent light microscopy (not shown). WONV infection was conducted at an MOI of 0.1 $TCID_{50}$/cell (F) or MOIs of 0.1 $TCID_{50}$/cell and 1.0 $TCID_{50}$/cell (G). Statistical analyses were conducted by using two-way analysis of variance with Tukey's multiple-comparison test to determine individual *P* values (A to E) or an unpaired, two-tailed Student *t* test (F) (GraphPad Prism 6C). Significant differences are indicated (****, $P \leq 0.0001$; ***, $P \leq 0.001$; **, $P \leq 0.01$; *, $P \leq 0.05$; NS, not significant).

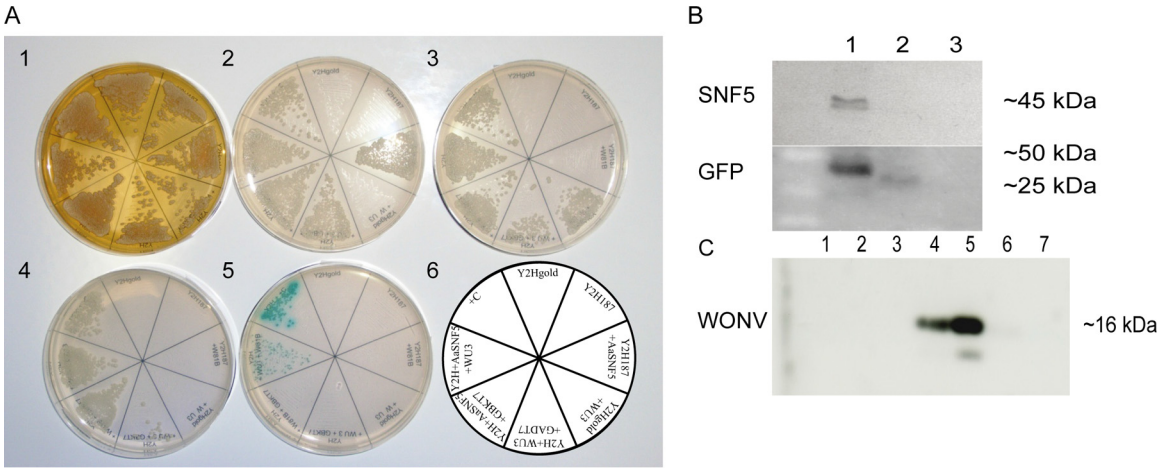

FIG 5 WONV U3 interacts with the full-length SNF5 from insect and mammalian cells. (A) Yeast two-hybrid analysis of the interaction between AaSNF5 and WONV U3. *S. cerevisiae* strain Y2H187 transformed with either pGADT7 alone or pGADT7(AaSNF5) was mated with the *S. cerevisiae* strain Y2HGold containing either pGBKT7 or pGBKT7(WU3). The resulting yeast strains were streaked out on (1) yeast peptone dextrose adenine medium (YPDA), (2) synthetic complete (SC) medium without leucine (SC^{-leu}), (3) SC medium without tryptophan (SC^{-trp}), (4) SC medium without leucine or tryptophan ($SC^{-leu/-trp}$), and (5) SC medium without leucine, tryptophan, histidine, or adenine ($SC^{-leu/-trp/-his/-ade}$) + 5-bromo-4-chloro-3-indolyl-α-D-galactopyranoside (X-α-Gal) + aurobasidin A to select for a true interaction. (B) Immunoblots using antibodies specific to SNF5 and GFP of the GFP binding fractions from lysates of BHK-BSR cells transfected with pAcGFP1-C2(WU3) (lane 1), pAcGFP1-C2 (lane 2), and no plasmid vector (lane 3). (C) Immunoblot of pulldown assay fractions demonstrating that WONV U3 expressed in WONV-infected Vero cells binds *in vitro* to the 84-aa C-terminal end of AaSNF5. Lane 1, MBP alone; lane 2, MBP plus a 38-hpi extract from WONV-infected Vero cells; lane 3, MBP/SNF5 alone; lane 4, MBP/SNF5 plus a 38-hpi extract from WONV-infected Vero cells; lane 5, 38-hpi extract from WONV-infected Vero cells; lane 6, 14-hpi extract from WONV-infected Vero cells; lane 7, extract from uninfected Vero cells. The immunoblot was probed with polyclonal anti-WU3 chicken antiserum.

clear fluorescence observed in COS-7 cells transfected with plasmid pAcGFP1-C2(WU3) increased following treatment with LMB, which inhibits nuclear protein export by the exportin CRM1 (17) (Fig. 6C). To quantify the nuclear localization of the proteins, Fn/c was determined for GFP and GFP-WU3 in cells at 27 h posttransfection, which indicated that the localization of WU3-GFP was significantly greater than that of GFP alone and showed a further significant increase following LMB treatment (Fig. 6D). Thus, it appears that WONV U3 can accumulate in the nucleus and that its nucleocytoplasmic localization is regulated by active nuclear export by CRM1. Similar results were observed following transfection of COS-7 cells with pEGFP-C1-RVP-P1 expressing the rabies virus P protein, which was shown previously to be trafficked into and out of the nucleus (13).

AaSNF5 expression is upregulated during infection of C6/36 cells with WNV, BEFV, and WONV. SNF5 expression was assessed by qRT-PCR following infection of C6/36 cells with WONV, BEFV, or WNV (MOI of 1 $TCID_{50}$/cell). As shown in Fig. 7A, a transient upregulation of SNF5 expression was observed at 9 hpi for each virus, and expression levels returned to normal by 24 hpi. The level of SNF5 induction varied from ~4-fold for WNV to ~2.5-fold for WONV.

AaSNF5 knockdown favors WONV replication. The effect of SNF5 knockdown on WONV infection was also assessed. C6/36 and BHK-BSR cells were transfected with double-stranded siRNA targeting SNF5 gene transcripts and then infected with 1 $TCID_{50}$/cell of WONV at 6 h posttransfection. Relative to control luciferase siRNA, treatment with SNF5 siRNA resulted in a significant reduction in SNF mRNA levels at 24 h posttransfection (Fig. 7B and D). siRNA-induced SNF5 knockdown resulted in a small but significant (~0.5 log $TCID_{50}$/ml) increase in WONV titers in both C6/36 and BHK-BSR cells (Fig. 7C and E). SNF5 knockdown was confirmed by immunoblotting at 24 h posttransfection (Fig. 7F).

WONV U3 inhibits SNF5-regulated gene expression. SNF5 has been shown to be involved in the transcriptional regulation of the colony-stimulating factor 1 gene (*CSF1*) in mammalian cells (18). To assess the effect of WONV U3 on SNF5-regulated gene expression, Vero and BHK-BSR cells were mock infected or infected with 1 $TCID_{50}$/cell WONV and transfected with pAcGFP1-C2(WU3) or control vector pAcGFP1-C2 at 6 hpi, and *CSF1* expression was analyzed at 48 h posttransfection. In each cell line, WONV U3 overexpression resulted in a significant reduction in *CSF1* transcript levels compared to those in control untreated cells (Fig. 8). Furthermore, WONV infection led to a significant reduction in *CSF1* transcript levels compared to those in control cells, while the overexpression of WONV U3 in the presence of WONV infection resulted in a significantly greater reduction of *CSF1* transcript levels. The effects of overexpression of WONV U3 and WONV infection were significantly greater in BHK-BSR cells than in Vero cells. In BHK-BSR cells, CSF1 transcript levels were >80% lower than those in control cells following WONV infection and >90% lower than those in control cells following WONV infection in the presence of overexpressed WONV U3. This was reflected in WONV infection levels, as determined by N gene transcript levels, which were ~10-fold higher in BHK-BSR cells than in Vero cells (not shown). These data indicate that WONV infection and overexpression of WONV U3 inhibit SNF5-regulated expression of CSF1.

DISCUSSION

The evolutionarily conserved SWI/SNF chromatin remodeling complex (also known as the BAF complex) plays a crucial role in the regulation of gene expression in eukaryote cells and is essential for proper development (19–21). It comprises 10 to 12 proteins, including an invariant core complex and variable subunits that regulate the transcription of target genes by the ATP-dependent

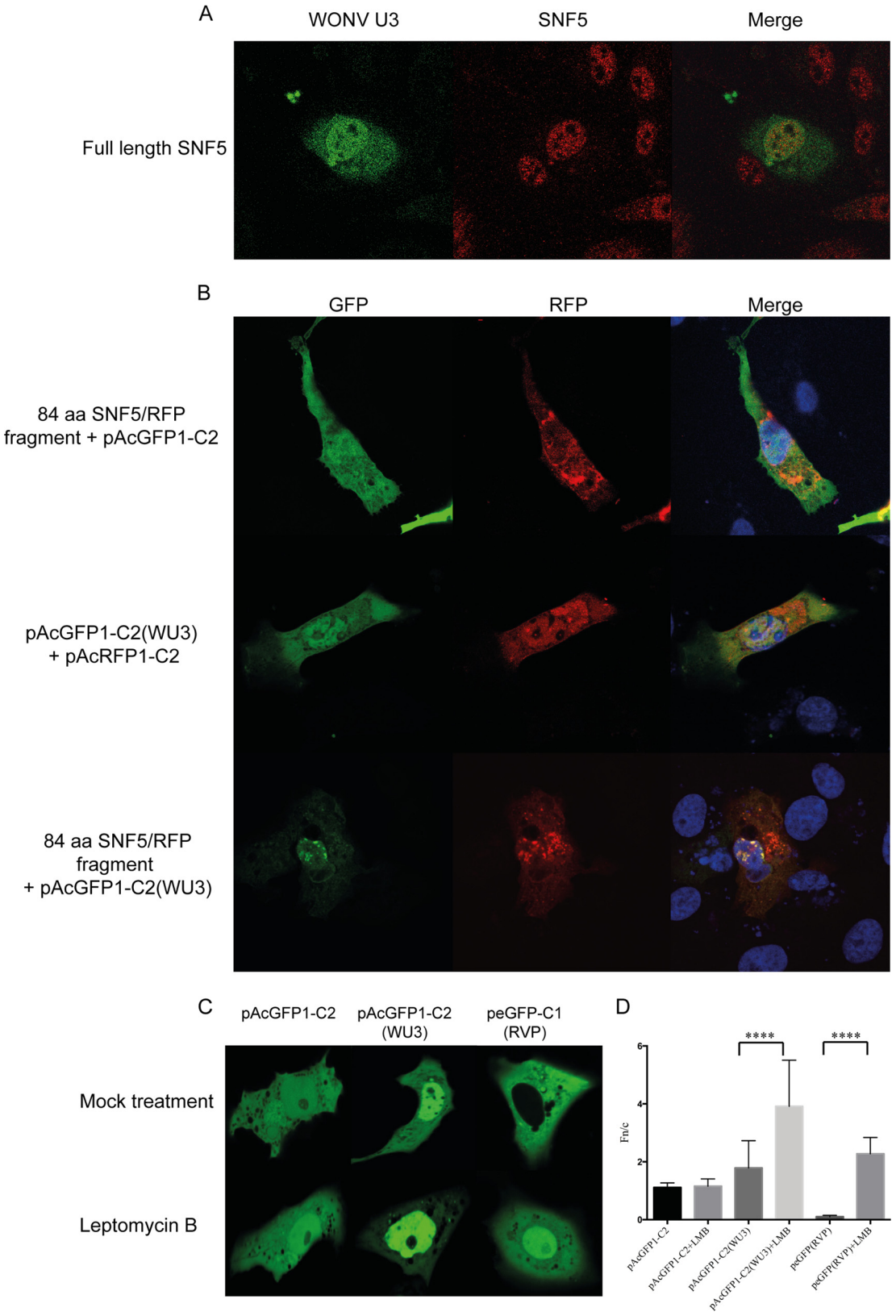

FIG 6 WONV U3 colocalizes with SNF5 in the nucleus and is actively exported from the nucleus via CRM1. (A) Confocal image of BHK-BSR cells infected with WONV showing WONV U3 (labeled green) and SNF5 (labeled red) colocalizing in the nucleus. (B) Confocal images demonstrating colocalization of AaSNF5 (red) and WONV U3 (green) in Vero cells transfected with plasmids pAcRFP-C2(SNF5) and pAcGFP-C2(WU3), respectively. Cells were cotransfected with plasmids expressing WU3-GFP and AaSNF5-RFP fusion proteins (84-aa C-terminal domain) and were imaged at 24 h posttransfection. (C) Confocal images of COS-7 cells transfected with pAcGFP1-C2, pAcGFP1-C2(WU3), and pEGFP-C1-RVP-P1 and treated with leptomycin B at 24 h posttransfection. (D) Images such as those shown in panel A were used to calculate the ratio of nuclear to cytoplasmic fluorescence (Fn/c), as previously described (13) ($n > 30 \pm$ standard errors of the means). Statistical analyses were conducted by using an ordinary one-way analysis of variance with Tukey's multiple-comparison test to determine specific *P* values by using GraphPad Prism 6C. Significant differences are indicated (****, $P \leq 0.0001$).

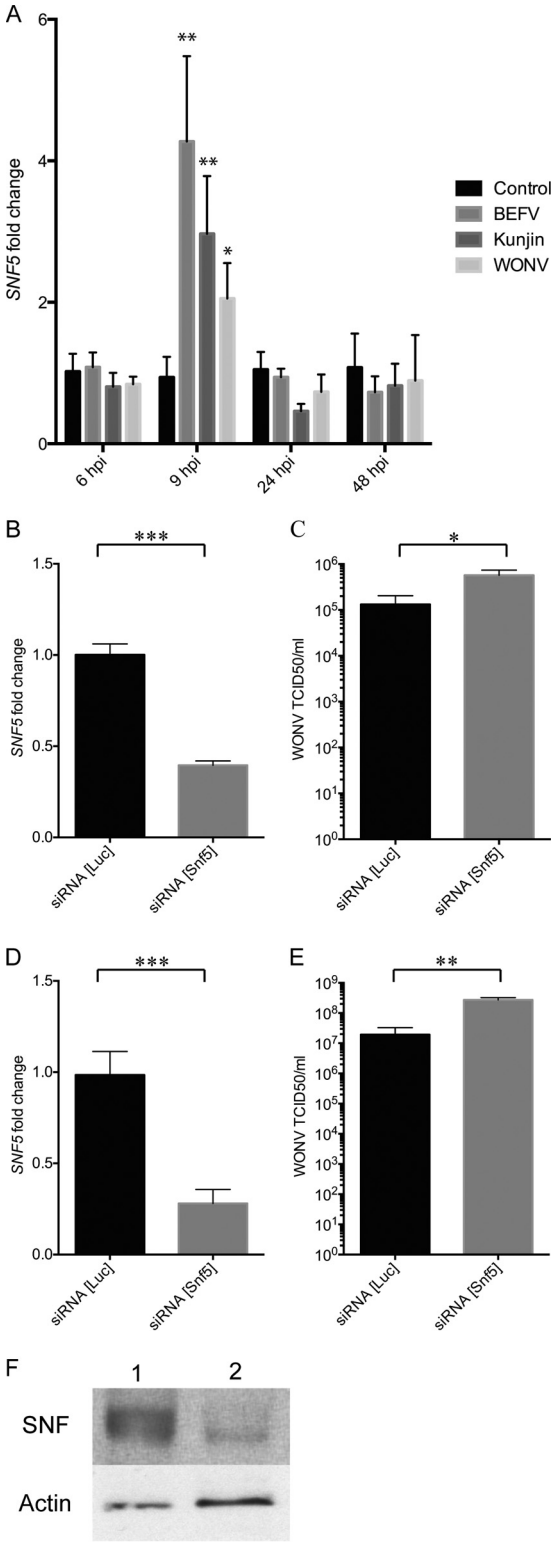

FIG 7 SNF5 modulates WONV replication in C6/36 and BHK-BSR cells. (A) SNF5 mRNA induction in C6/36 cells at 6 h, 24 h, 48 h, and 72 h after infection with WNV, BEFV, and WONV. *SNF5* expression levels were determined by qRT-PCR and are shown as fold induction values with respect to mock-infected cells at the same time point. (B and C) *SNF5* mRNA quantification by qRT-PCR (B) and WONV $TCID_{50}$ titers (C) in C6/36 cells transfected with siRNA directed against the luciferase control (siRNA[Luc]) or SNF5 (siRNA[Snf5]) and infected with WONV at 6 h posttransfection. (D and E) SNF5 mRNA quantification by qRT-PCR (D) and WONV $TCID_{50}$ titers (E) in BHK-BSR cells transfected with siRNA[Luc] or siRNA[Snf5] and infected with WONV at 6 h posttransfection. (F) Immunoblots from BHK/BSR cell lysates transfected with siRNA[Luc] (lane 1) or siRNA[SNF5] (lane 2). The immunoblots were probed with SNF5 antibody and actin antibody (Abcam). Assays were conducted at 24 h posttransfection. $TCID_{50}$ titrations were performed in Vero cells. Statistical analysis for panel A was conducted by using two-way analysis of variance with Tukey's multiple-comparison test to determine individual *P* values. Statistical analysis for panels B to E was done by using an unpaired *t* test with equal standard deviations (GraphPad Prism 6C). Significant differences are indicated (***, $P \leq 0.001$; **, $P \leq 0.01$; *, $P \leq 0.05$).

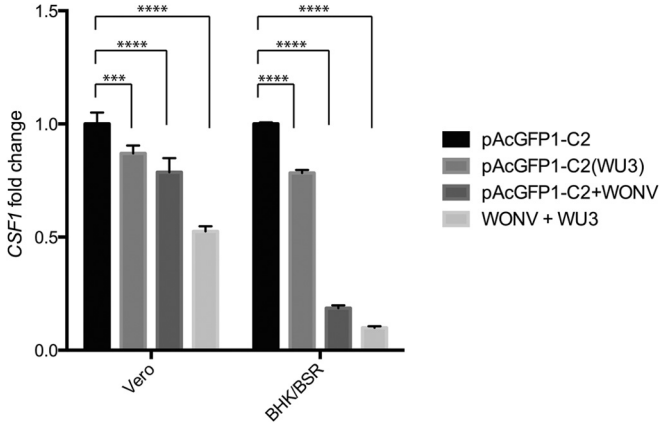

FIG 8 Colony-stimulating factor 1 gene (*CSF1*) transcript levels in Vero cells or BHK-BSR cells following overexpression of WONV U3 and infection with 1 $TCID_{50}$/ml of WONV. Statistical analyses were conducted by using an ordinary one-way analysis of variance with Tukey's multiple-comparison test to determine specific *P* values (GraphPad Prism 6C). Significant differences are indicated (****, $P \leq 0.0001$; ***, $P \leq 0.001$).

mobilization of nucleosomes and chromatin remodeling. Loss of SWI/SNF function has been associated with malignant transformation, and several components of the complex appear to act as tumor suppressors (22, 23). The SWI/SNF complex has also been shown to be required for the transcriptional activation of the cytokine CSF1 (18, 24) as well as the majority of type I interferon (IFN)-inducible genes and plays an essential role in the antiviral response of mammalian cells (25). SNF5 (also known as INI1, BAP47, and Smarcb1) is a key component of the core SWI/SNF complex. It contains three highly conserved regions: dual imperfect repeat domains, the second of which includes a masked nuclear export signal (NES), and a moderately conserved C-terminal coiled-coiled region assigned as the homology region 3 (HR3) domain (18, 26, 27) (Fig. 4). SNF5 appears to recruit the SWI/SNF complex to specific sites in chromatin through interactions with various transcriptional regulatory proteins. Knockdown of SNF5 has been shown to suppress the activation of the IFN-β response and enhance the replication of Newcastle disease virus in HeLa cells (25).

In this paper, we have shown that the WONV accessory protein U3 is expressed during infection in mammalian cells and insect cells, is essential for efficient virus replication, and specifically interacts with the 83-aa C-terminal domain of SNF5. In mammalian cells, WONV U3 colocates with SNF5 in the nucleus and blocks SNF5-regulated gene expression. In insect cells, SNF5 is upregulated in response to infection with WONV (as well as other arthropod-borne viruses, including the rhabdovirus BEFV and the fla-

vivirus WNV), and inhibition of SNF5 expression by siRNA knockdown favors WONV replication. Overall, our data indicate that WONV U3 has a crucial facilitating role during infection in both mammalian cells and insect cells through its interaction with SNF5.

There are several previous reports of the interaction of SNF5 with viral proteins. Human papillomavirus 18 (HPV-18) E1 and E2 proteins have been shown to recruit SNF5, stimulating viral transcriptional activation and DNA replication (28, 29). Epstein-Barr virus nuclear antigen 2 (EBNA2) binds to SNF5 in a process that appears to be related to the immortalization of B cells (30, 31), and the K8 protein of Kaposi's sarcoma-associated herpesvirus interacts with the N-terminal half of SNF5 to facilitate transcriptional activation (32). HIV-1 integrase also interacts with SNF5 in both the nucleus and the cytoplasm of infected T cells and is incorporated into mature virions (33, 34). However, to our knowledge, there is no previous report of SNF5 interaction with RNA viruses (other than retroviruses), and our study appears to provide the first evidence of a virus targeting SNF5 to inhibit host gene expression. We have used *CSF1* as a marker of SWI/SNF-regulated gene expression, as SNF5 has been clearly shown to be required for its transcriptional activation (18, 24), and it is an important regulator of immune responses (35). Although *CSF1* expression is shown here to be inhibited by WONV U3, further work is required to determine if the WONV U3/SNF5 interaction is specifically targeting host antiviral defenses. The interaction with SNF5 is of particular interest for insect cells, which lack an interferon response but appear to employ a parallel Jak-STAT-mediated antiviral defensive pathway (36).

WONV U3 was found to accumulate in the nucleus by laser scanning confocal microscopy, and the nuclear localization was significantly enhanced by treatment with LMB, a specific inhibitor of the nuclear export receptor protein CRM1, indicating that WONV U3 enters the nucleus and is actively transported out of the nucleus. Indeed, we identified sequences in WONV U3 consistent with a nuclear localization signal (NLS) and an NES, both within the N-terminal domain (see http://nls-mapper.iab.keio.ac.jp/cgi-bin/NLS_Mapper_form.cgi and http://www.cbs.dtu.dk/services/NetNES), and so trafficking of WONV U3 may occur through direct interactions with karyopherins. However, as the WU3-GFP fusion protein (~43.4 kDa) does not exceed the nuclear exclusion limit, entry into the nucleus may be possible by diffusion. Furthermore, as SNF5 has also been shown to be actively trafficked both into and out of the nucleus, it is also possible that the subcellular localization of WONV U3 is mediated, at least in part, by its interaction with SNF5. At present, we have no direct evidence for independent trafficking of WONV U3, and this requires further investigation.

The yeast two-hybrid assay established that WONV U3 specifically interacts with the 83-aa C-terminal region of SNF5. This comprises primarily the predicted coiled-coil region identified previously by Morozov et al. (27) and a portion of repeat region II downstream of the masked NES. The function of the coiled-coil region is currently unknown, but it is highly conserved across eukaryote SNF5 orthologs. Indeed, this region is almost perfectly conserved among primate, rodent, and avian SNF5 orthologs, and there is extensive homology between the vertebrate and insect orthologs (Fig. 4). Evidence presented here showing that WONV U3 can bind to SNF5 in both vertebrate and mosquito cells suggests that it may perform similar functions by interacting with the SWI/SNF complex during infection of both vertebrate hosts and vectors. The SWI/SNF complex is known to regulate the expression of vertebrate immune response genes (18, 25), and this is supported by our experimental evidence that WONV U3 blocks the expression of the SWI/SNF-regulated cytokine CSF. Although we have not yet assessed the consequences of the WONV U3/SNF interaction in insect cells, the possibility that it may also subvert the antiviral response in the vector may provide useful insights into this largely neglected aspect of the arbovirus transmission cycle.

The role of the other small accessory proteins encoded in ORFs located in succession between the WONV P and M genes also requires investigation. WONV ORFs U1 and U2 encode proteins of a size similar to that of WONV U3, and their deduced amino acid sequences display a high level of overall sequence similarity and several short regions of high pairwise sequence identity (6). Each ORF is bounded by putative transcription initiation (GUCA) and transcription termination/polyadenylation (G[U/A]ACUUUUUUU) sequences, indicating that they are likely to be transcribed and expressed during infection (1, 6). However, WONV U1 and WONV U2 lack the characteristic asparagine-rich C-terminal domain of WONV U3, and there is no evidence of an NLS in either protein. Interestingly, WU1 is predicted to contain an NES in the N-terminal domain, suggesting that it may indeed have a nuclear function. In rabies virus, various isoforms of the P protein (P1 to P5) are generated by leaky ribosomal scanning, and they accumulate differently in the cell due to an NES in the N-terminal domain and an NLS in the C-terminal domain of the full-length protein (37–39). The P isoforms antagonize the interferon response by various mechanisms, including the sequestration of STAT1 out of the nucleus (40). It would be of interest to determine if the three small WONV accessory proteins also act in concert to subvert the cellular antiviral response.

Over the past several decades, intensive molecular studies of rhabdoviruses have focused largely on rabies virus and vesicular stomatitis virus, which have served as general models not only for understanding rhabdoviruses but also more broadly for understanding the structure and function of nonsegmented negative-sense RNA viruses. However, it is becoming increasingly evident that the genome organizations and expression strategies displayed by these well-known prototypes are not representative of many rhabdoviruses, which, in addition to the five structural proteins (N, P, M, G, and L), commonly contain a diverse array of additional ORFs encoding putative accessory proteins of unknown function. Many of these proteins are likely to have important roles in pathogenesis and in modulating the host response to infection. Exploration of their functions not only may reveal the diversity of strategies employed by viruses to engage the host but also has the potential to expose fundamental aspects of cell biology that are currently unknown. Of particular interest is the role of viral accessory proteins in insect cells, for which little is known of the processes of infection and immunity.

ACKNOWLEDGMENTS

We acknowledge Lee Trinidad and Cassandra David for technical assistance and the facilities and technical assistance of Monash Micro Imaging, Victoria, Australia.

We thank David Jans for supplying cells.

The study was supported in part by a grant from the National Health and Medical Research Council of Australia (grant 1003244) to G.W.M.

REFERENCES

1. **Walker PJ, Dietzgen RG, Joubert DA, Blasdell KR.** 2011. Rhabdovirus accessory genes. Virus Res **162:**110–125. http://dx.doi.org/10.1016/j.virusres.2011.09.004.
2. **Garcia-Sastre A.** 2001. Inhibition of interferon-mediated antiviral responses by influenza A viruses and other negative-strand RNA viruses. Virology **279:**375–384. http://dx.doi.org/10.1006/viro.2000.0756.
3. **Karjee S, Minhas A, Sood V, Ponia SS, Banerjea AC, Chow VT, Mukherjee SK, Lal SK.** 2010. The 7a accessory protein of severe acute respiratory syndrome coronavirus acts as an RNA silencing suppressor. J Virol **84:**10395–10401. http://dx.doi.org/10.1128/JVI.00748-10.
4. **Koetzner CA, Kuo L, Goebel SJ, Dean AB, Parker MM, Masters PS.** 2010. Accessory protein 5a is a major antagonist of the antiviral action of interferon against murine coronavirus. J Virol **84:**8262–8274. http://dx.doi.org/10.1128/JVI.00385-10.
5. **Ammar E-D, Tsai CW, Whitfield AE, Redinbaugh MG, Hogenhout SA.** 2009. Cellular and molecular aspects of rhabdovirus interactions with insect and plant hosts. Annu Rev Entomol **54:**447–468. http://dx.doi.org/10.1146/annurev.ento.54.110807.090454.
6. **Gubala AJ, Proll DF, Barnard RT, Cowled CJ, Crameri SG, Hyatt AD, Boyle DB.** 2008. Genomic characterisation of Wongabel virus reveals novel genes within the *Rhabdoviridae*. Virology **376:**13–23. http://dx.doi.org/10.1016/j.virol.2008.03.004.
7. **Humphery-Smith I, Cybinski DH, Byrnes KA, St George TD.** 1991. Seroepidemiology of arboviruses among seabirds and island residents of the Great Barrier Reef and Coral Sea. Epidemiol Infect **107:**435–440. http://dx.doi.org/10.1017/S0950268800049086.
8. Reference deleted.
9. **Blasdell KR, Voysey R, Bulach DM, Trinidad L, Tesh RB, Boyle DB, Walker PJ.** 2012. Malakal virus from Africa and Kimberley virus from Australia are geographic variants of a widely distributed ephemerovirus. Virology **433:**236–244. http://dx.doi.org/10.1016/j.virol.2012.08.008.
10. **Joubert DA, Blasdell KR, Audsley MD, Trinidad L, Monaghan P, Dave KA, Lieu K, Amos-Ritchie R, Jans DA, Moseley GW, Gorman JJ, Walker PJ.** 2014. Bovine ephemeral fever rhabdovirus a1 protein has viroporin-like properties and binds importin b1 and importin 7. J Virol **88:**1591–1603. http://dx.doi.org/10.1128/JVI.01812-13.
11. **Reed LJ, Muench H.** 1938. A simple method of estimating fifty percent endpoints. Am J Hyg **27:**493–497.
12. **Ren B, Pham TM, Surjadi R, Robinson CP, Le TK, Chandry PS, Peat TS, McKinstry WJ.** 2013. Expression, purification, crystallization and preliminary X-ray diffraction analysis of a lactococcal bacteriophage small terminase subunit. Acta Crystallogr Sect F Struct Biol Cryst Commun **69:**275–279. http://dx.doi.org/10.1107/S174430911300184X.
13. **Moseley GW, Roth DM, DeJesus MA, Leyton DL, Filmer RP, Pouton CW, Jans DA.** 2007. Dynein light chain association sequences can facilitate nuclear protein import. Mol Biol Cell **18:**3204–3213. http://dx.doi.org/10.1091/mbc.E07-01-0030.
14. **Vandesompele J, De Preter K, Pattyn F, Poppe B, Van Roy N, De Paepe A, Speleman F.** 2002. Accurate normalization of real-time quantitative RT-PCR data by geometric averaging of multiple internal control genes. Genome Biol **3:**RESEARCH0034. http://dx.doi.org/10.1186/gb-2002-3-7-research0034.
15. **Jagani Z, Mora-Blanco EL, Sansam CG, McKenna ES, Wilson B, Chen D, Klekota J, Tamayo P, Nguyen PT, Tolstorukov M, Park PJ, Cho YJ, Hsiao K, Buonamici S, Pomeroy SL, Mesirov JP, Ruffner H, Bouwmeester T, Luchansky SJ, Murtie J, Kelleher JF, Warmuth M, Sellers WR, Roberts CW, Dorsch M.** 2010. Loss of the tumor suppressor Snf5 leads to aberrant activation of the Hedgehog-Gli pathway. Nat Med **16:**1429–1433. http://dx.doi.org/10.1038/nm.2251.
16. **Xu Y, Yan W, Chen X.** 2010. SNF5, a core component of the SWI/SNF complex, is necessary for p53 expression and cell survival, in part through eIF4E. Oncogene **29:**4090–4100. http://dx.doi.org/10.1038/onc.2010.159.
17. **Fornerod M, Ohno M, Yoshida M, Mattaj IW.** 1997. CRM1 is an export receptor for leucine-rich nuclear export signals. Cell **90:**1051–1060. http://dx.doi.org/10.1016/S0092-8674(00)80371-2.
18. **Pan X, Song Z, Zhai L, Li X, Zeng X.** 2005. Chromatin-remodeling factor INI1/hSNF5/BAF47 is involved in activation of the colony stimulating factor 1 promoter. Mol Cells **20:**183–188.
19. **Cairns BR.** 1998. Chromatin remodeling machines: similar motors, ulterior motives. Trends Biochem Sci **23:**20–25. http://dx.doi.org/10.1016/S0968-0004(97)01160-2.
20. **Simone C.** 2006. SWI/SNF: the crossroads where extracellular signaling pathways meet chromatin. J Cell Physiol **207:**309–314. http://dx.doi.org/10.1002/jcp.20514.
21. **Ho L, Crabtree GR.** 2010. Chromatin remodelling during development. Nature **463:**474–484. http://dx.doi.org/10.1038/nature08911.
22. **Roberts CW, Orkin SH.** 2004. The SWI/SNF complex—chromatin and cancer. Nat Rev Cancer **4:**133–142. http://dx.doi.org/10.1038/nrc1273.
23. **Euskirchen G, Auerbach RK, Snyder M.** 2012. SWI/SNF chromatin-remodeling factors: multiscale analyses and diverse functions. J Biol Chem **287:**30897–30905. http://dx.doi.org/10.1074/jbc.R111.309302.
24. **Liu R, Liu H, Chen X, Kirby M, Brown PO, Zhao K.** 2001. Regulation of CSF1 promoter by the SWI/SNF-like BAF complex. Cell **106:**309–318. http://dx.doi.org/10.1016/S0092-8674(01)00446-9.
25. **Cui K, Tailor P, Liu H, Chen X, Ozato K, Zhao K.** 2004. The chromatin-remodeling BAF complex mediates cellular antiviral activities by promoter priming. Mol Cell Biol **24:**4476–4486. http://dx.doi.org/10.1128/MCB.24.10.4476-4486.2004.
26. **Craig E, Zhang Z-K, Davies KP, Kalpana GV.** 2002. A masked NES in INI1/hSNF5 mediates hCRM1-dependent nuclear export: implications for tumorigenesis. EMBO J **21:**31–42. http://dx.doi.org/10.1093/emboj/21.1.31.
27. **Morozov A, Yung E, Kalpana GV.** 1998. Structure-function analysis of integrase interactor 1/hSNF5L1 reveals differential properties of two repeat motifs present in the highly conserved region. Proc Natl Acad Sci U S A **95:**1120–1125. http://dx.doi.org/10.1073/pnas.95.3.1120.
28. **Lee D, Sohn H, Kalpana GV, Choe J.** 1999. Interaction of E1 and hSNF5 proteins stimulates replication of human papillomavirus DNA. Nature **399:**487–491. http://dx.doi.org/10.1038/20966.
29. **Cha S, Seo T.** 2011. hSNF5 is required for human papillomavirus E2-driven transcriptional activation and DNA replication. Intervirology **54:**66–77. http://dx.doi.org/10.1159/000318871.
30. **Wu DY, Kalpana GV, Goff SP, Schubach WH.** 1996. Epstein-Barr virus nuclear protein 2 (EBNA2) binds to a component of the human SNF-SWI complex, hSNF5/Ini1. J Virol **70:**6020–6028.
31. **Kwiatkowski B, Chen SYJ, Schubach WH.** 2004. CKII site in Epstein-Barr virus nuclear protein 2 controls binding to hSNF5/Ini1 and is important for growth transformation. J Virol **78:**6067–6072. http://dx.doi.org/10.1128/JVI.78.11.6067-6072.2004.
32. **Hwang S, Lee D, Gwack Y, Min H, Choe J.** 2003. Kaposi's sarcoma-associated herpesvirus K8 protein interacts with hSNF5. J Gen Virol **84:**665–676. http://dx.doi.org/10.1099/vir.0.18699-0.
33. **Kalpana G, Marmon S, Wang W, Crabtree G, Goff S.** 1994. Binding and stimulation of HIV-1 integrase by a human homolog of yeast transcription factor SNF5. Science **266:**2002–2006. http://dx.doi.org/10.1126/science.7801128.
34. **Yung E, Sorin M, Wang E-J, Perumal S, Ott D, Kalpana GV.** 2004. Specificity of interaction of INI1/hSNF5 with retroviral integrases and its functional significance. J Virol **78:**2222–2231. http://dx.doi.org/10.1128/JVI.78.5.2222-2231.2004.
35. **Sweet MJ, Hume DA.** 2003. CSF-1 as a regulator of macrophage activation and immune responses. Arch Immunol Ther Exp (Warsz) **51:**169–177.
36. **Paradkar PN, Trinidad L, Voysey R, Duchemin JB, Walker PJ.** 2012. Secreted Vago restricts West Nile virus infection in Culex mosquito cells by activating the Jak-STAT pathway. Proc Natl Acad Sci U S A **109:**18915–18920. http://dx.doi.org/10.1073/pnas.1205231109.
37. **Chenik M, Chebli K, Blondel D.** 1995. Translation initiation at alternate in-frame AUG codons in the rabies virus phosphoprotein mRNA is mediated by a ribosomal leaky scanning mechanism. J Virol **69:**707–712.
38. **Moseley GW, Filmer RP, DeJesus MA, Jans DA.** 2007. Nucleocytoplasmic distribution of rabies virus P protein is regulated by phosphorylation adjacent to C-terminal nuclear import and export signals. Biochemistry **46:**12053–12061. http://dx.doi.org/10.1021/bi700521m.
39. **Pasdeloup D, Poisson N, Raux H, Gaudin Y, Ruigrok RW, Blondel D.** 2005. Nucleocytoplasmic shuttling of the rabies virus P protein requires a nuclear localization signal and a CRM1-dependent nuclear export signal. Virology **334:**284–293. http://dx.doi.org/10.1016/j.virol.2005.02.005.
40. **Moseley GW, Lahaye X, Roth DM, Oksayan S, Filmer RP, Rowe CL, Blondel D, Jans DA.** 2009. Dual modes of rabies P-protein association with microtubules: a novel strategy to suppress the antiviral response. J Cell Sci **122:**3652–3662. http://dx.doi.org/10.1242/jcs.045542.